

Mechanical Properties of the Shuttle Orbiter Thermal Protection System Strain Isolator Pad

James Wayne Sawyer*

NASA Langley Research Center, Hampton, Virginia

An experimental investigation has been conducted to determine the static and fatigue properties of the Strain Isolator Pad (SIP) used on the shuttle orbiter thermal protection system. Static tension-compression, and shear test results show that the SIP is highly nonlinear, has a large hysteresis, a large low-modulus region for low stress levels, and stress-strain properties that are highly sensitive to strain rate and previous load history. In addition, the shear properties are also sensitive to forces applied normal to the plane of the pad and to the orientation of the material. For the undensified tile/SIP system, static and fatigue failure occurs at the SIP/tile interface at low stress levels and for a small number of cycles. Densifying the faying surface of the tile improves the static strength and, to a lesser degree, the fatigue strength of the SIP/tile system. Although static failure occurs in the tile, cyclic loading causes excessive elongation or complete failure of the SIP at a relatively low fatigue life. Thus, the full benefit of the increased static strength of the densified tile system is not achieved in fatigue.

Introduction

THE aluminum skin of the space shuttle orbiter is protected against high temperatures by approximately 30,000 low density Reusable Surface Insulation (RSI) tiles. These tiles are relatively brittle, with a low coefficient of thermal expansion, and cannot be attached directly to the aluminum skin of the orbiter. The tiles are bonded to Nomex felt Strain Isolator Pads (SIP) which, in turn, are bonded to the aluminum skin of the orbiter. The SIP and tiles are bonded using a Room Temperature Vulcanizing (RTV) silicone rubber adhesive. The SIP material serves to isolate the fragile tile material from the relatively large deformations of the aluminum substructure which occur due to mechanical and thermal loads. A good understanding of the mechanical properties of the TPS materials is needed to evaluate the structural integrity of the TPS.

An investigation was undertaken to determine the tensile, compression, and shear mechanical properties and fatigue properties of the TPS materials. These properties are needed to evaluate the stress levels and motion of the tiles and to determine the expected life of the TPS system. Limited tests were performed on the RSI tiles, RTV adhesive, and the SIP to study the material response to various load conditions. Improved fixtures and test techniques were employed to obtain realistic material response. Results of these tests indicated that the flexibility of the SIP material is the primary factor in determining the response of the TPS to the flight loads. The present paper summarizes the limited static and fatigue results obtained for the SIP material and the SIP/tile combined structure. For more detail of the tests, see Refs. 1-3.

SIP Description

The SIP is a felt pad that is bonded between the RSI tile and the aluminum primary structure of the shuttle orbiter. The pad is necessary to isolate the rigid tiles from strains due to thermal expansion of the orbiter structure and skin deflections due to aerodynamic loads. The SIP is a mat of randomly

oriented horizontal Nomex fibers. During manufacture, the mat is passed through a series of needled rollers which compress the mat and reorient a few of the fibers transverse to the plane of the mat. The transverse fibers hold the mat together and provide a mechanism for transferring loads from the tile to the aluminum skin.

Results of an investigation on the microstructure of the SIP were reported in Ref. 4 and typical photomicrographs from that report are shown in Fig. 1. Figures 1a and 1b are views of the face of the SIP. At low magnification (Fig. 1a), a pattern of dimples can be seen on the face of the SIP. The highly magnified view (Fig. 1b) shows that the dimples are locations of transverse bundles. Figure 1c shows a cross-section view of the SIP and the orientation of the transverse bundles through the SIP thickness. The RTV adhesive transfer coating shown in Fig. 1c was developed to aid in bonding the SIP to the RSI tile. However, not all the transverse fibers are securely locked into the transfer coat. The transverse fiber bundles are not perpendicular to the plane of the SIP and are generally slanted in one direction, depending on the rolling direction of the material. Thus, the SIP material has a preferred orientation and a shear-extension coupling. Transverse fiber bundles also introduce stress concentrations⁵ which cause premature failures in the tile at the RSI/SIP interface. A process for densifying the faying surface of the tile has been developed which greatly increases the strength of the SIP/tile system.^{6,7}

Specimens and Tests

Specimens

Two types of specimens were used in the present investigation. A pokerchip specimen was used to determine the static tension and compression characteristics of the SIP material and to determine the cyclic fatigue behavior of the SIP/RSI system. A double lap joint specimen was used to determine the static shear characteristics of the SIP material. All specimens were made following a procedure that is a close duplicate of that used on the actual orbiter. To insure that the adhesive had cured sufficiently, a Shore hardness of 50 or greater was required before testing the specimens.

Material

The materials considered in this investigation include both the 0.41 cm (0.160 in.) and 0.23 cm (0.090 in.) thick SIP in wide use on the orbiter, RTV-560 adhesive, and for the cyclic

Presented as Paper 82-0789 at the AIAA/ASME/ASLE/AHS 23rd Structures, Structural Dynamics and Materials Conference, New Orleans, La., May 10-12, 1982; submitted July 26, 1982; revision received Oct. 7, 1983. This paper is declared a work of the U.S. Government and therefore is in the public domain.

*Aerospace Engineer, Structures and Dynamics Division.

fatigue specimens, both the LI-900 and LI-2200 densified and undensified RSI tiles. The RTV-560 is a room temperature vulcanizing silicone rubber adhesive which is used to form a transfer coat on one side of the SIP and to bond the SIP to the RSI tiles and the orbiter skin. The RSI tiles are made of rigidized silica fibers. The LI-900 RSI has a density of 145 kg/m^3 (9 lb/ft^3). The LI-2200 RSI has a density of 354 kg/m^3 (22 lb/ft^3). For some of the tests, the tiles were densified by brushing a controlled amount of ceramic slurry on the tile surface next to the SIP/tile interface. The slurry is a mixture of colloidal silica and a silica slip containing small particles of silica. On drying, this mixture provides a hard, strong, densified layer approximately 0.25 cm (0.10 in.) thick.

The SIP and tile material were obtained from the same supply as that for the shuttle. The SIP was obtained with a 0.013 cm (0.005 in.) thick RTV-560 transfer coat applied to one side and cured. Fresh RTV-560 was obtained from the manufacturer to insure that the shelf life had not been exceeded. All specimen support fixtures were made from 2024-T4 aluminum. Aluminum fixture surfaces that were to be bonded to test specimens were prepared according to the procedure used on the shuttle orbiter—chemically etched, sprayed with a protective primer (Koropon), and vacuum baked to remove all volatiles.

Tension Specimen Configuration

Detail dimensions of the SIP pokerchip test specimen used for the static tension/compression tests are given in Fig. 2. The SIP is bonded between two aluminum blocks 5.72 cm (2.25 in.) in diameter with a 0.80 cm (0.31 in.) diameter alignment pin hole through the center. A 0.011 cm (0.004 in.) and 0.018 cm (0.007 in.) thick layer of RTV-560 adhesive is used to bond the transfer coated and uncoated sides of the SIP, respectively, to the aluminum blocks. An alignment pin is inserted through the center of the aluminum block and the test material while bonding and during the cure of the adhesive, but is removed before testing. Weights are used to apply the correct pressure to the joints during the cure.

Shear Specimen Configuration

As a result of the orientation of the SIP transverse fiber bundles, shear deformations also cause large deformations through the thickness of the pad (transverse normal direction). Thus, small transverse normal loads may significantly affect the measured shear characteristics of the material. The block shear tests, which would usually be considered for such a material, inherently have small normal forces present which may affect the measured shear properties. To avoid the inaccuracies caused by these small normal forces, a double lap shear joint has been used for the present tests. The doublers are free to move in the normal direction and, thus, do not introduce any external normal loads in the test material. Detailed dimensions of the double-lap joint test specimen are given in Fig. 3. Four identical pieces of SIP are bonded between the two aluminum adherends and the doublers. Relatively large [$6.35 \times 7.62 \text{ cm}$ ($2.5 \times 3.0 \text{ in.}$)] pieces of SIP are used to minimize edge effects. A 0.011 cm (0.004 in.) and 0.018 cm (0.007 in.) thick layer of RTV-560 is used to bond the transfer coated and uncoated sides of the SIP, respectively, to the aluminum. Tests were conducted with the shear load applied either parallel to or at right angles to the rolling direction of the material in order to obtain shear properties for both orientations.

Fatigue Specimen Configuration

The cyclic fatigue tests were conducted using a poker-chip specimen similar to that used for the static tension/compression tests but with RSI bonded to one side of the SIP (see Fig. 4). Tests were conducted for the 0.41 cm (0.160 in.) thick SIP with the LI-900 densified and undensified tiles and for the 0.23 cm (0.090 in.) thick SIP with the LI-2200

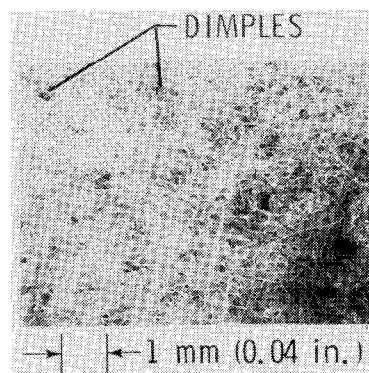


Fig. 1a Photomicrograph of SIP: uncoated SIP face.

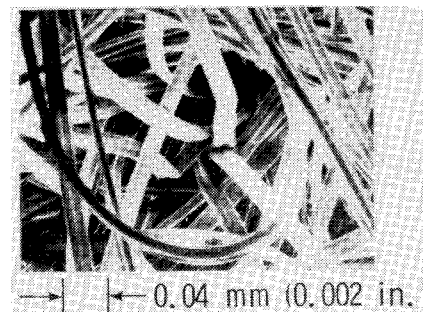


Fig. 1b Photomicrograph of SIP: dimple in SIP face.

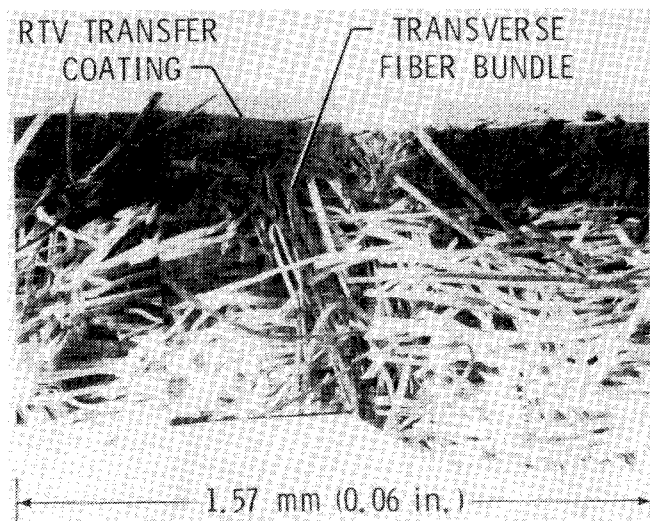


Fig. 1c Photomicrograph of SIP: cross-section of SIP.

densified and undensified tiles. For the densified tile specimens, the densified surface was bonded to the transfer coated side of the SIP. The tile material was 1.59 cm (0.62 in.) thick for the undensified tiles and 2.54 cm (1.0 in.) thick for the densified tiles.

Tests

All tests were conducted in a hydraulically actuated test machine that can be operated in either the load or displacement control mode. A 0.9 kN (200 lb) and 44 kN ($10,000 \text{ lb}$) tension/compression load cell were used for the pokerchip and shear specimens, respectively. Specimen axial displacement was measured using a displacement transducer which indicated testing machine head motion. For the shear tests, normal displacement of the doublers with respect to the adherends was measured, using displacement transducers mounted on the doublers. Data were recorded using an $x-y$ recorder and a digital data acquisition system.

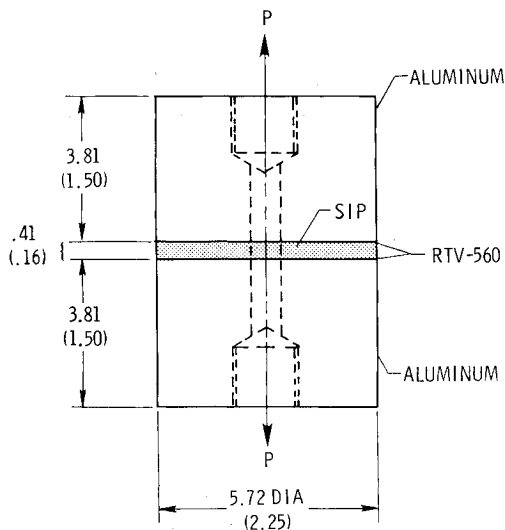


Fig. 2 Detail of SIP poker-chip test specimens. Dimensions given in cm (in.).

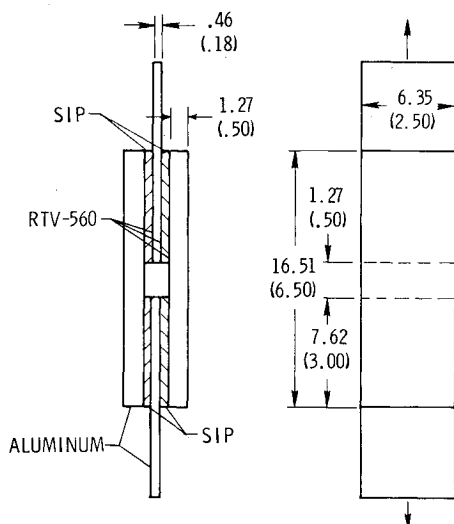


Fig. 3 Double lap joint SIP shear test specimen. Dimensions given in cm (in.).

The procedure followed in setting up a test was to zero the load cell with tare loads attached. The specimen was then installed with the test machine in the displacement control mode. After specimen installation, the test machine control mode was switched to load control which removed any residual setup loads that were applied to the SIP. The x-y recorder was then calibrated and the load and displacement scales zeroed.

Tension/Compression Tests

Tension/compression tests were conducted on virgin SIP material and material that had been subjected to various load conditions which are typical of those that would be experienced on the orbiter before and during the first flight. Most of the test specimens were load conditioned by giving them a static proof loading to simulate the maximum [69 kPa (10 psi)] proof tests performed on tiles installed on the orbiter. The proof load was applied and removed at the rate of 3.5 kPa (0.5 psi) per second. The loads were held constant for 30 s each at 6.9 kPa (1 psi) and 13.8 kPa (2 psi) below the maximum tensile proof load. The load was held constant for 60 s at the maximum tensile load and for 30 s at the maximum compression load. In addition to the proof loading, many specimens were load conditioned for a number of cycles to

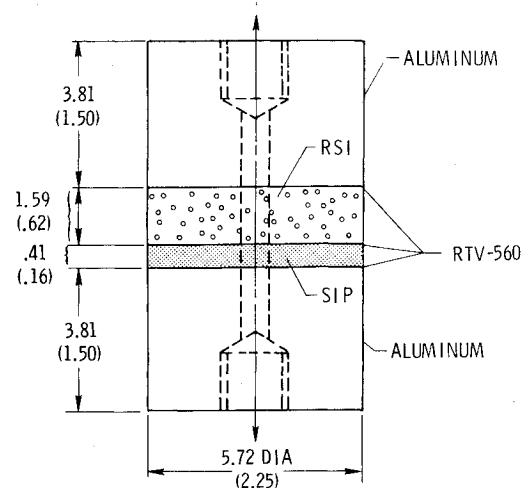


Fig. 4 Cyclic fatigue test specimen. Dimensions given in cm (in.).

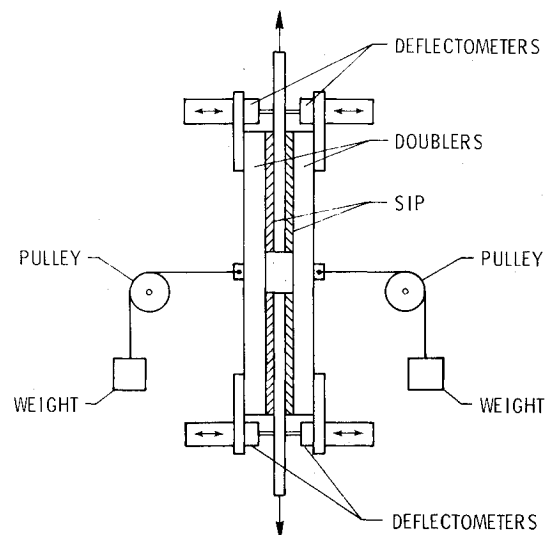


Fig. 5 SIP shear test setup with normal force applied to doublers.

approximate an accumulation of launch loads. The conditioning cycles were performed at 1 cycle per second (cps) with a fully reversed load of 80% of the proof load to approximate design load levels. Stress-strain data were obtained at a loading rate of 0.01 cps. Static ultimate tensile strengths were obtained at various load rates.

Shear Tests

The shear tests were conducted using the double lap joint by applying tension and compression loads to the metal adherends. The stress-strain curves were run at 0.01 cps with a sinusoidal load cycle. For some of the tests, the shear specimens were first load conditioned for a number of fully reversed sinusoidal cycles at a rate of 0.1 cps. Ultimate shear strengths were determined by applying a shear load at the rate of 1.5 kPa (0.2 psi) per s. A few tests were conducted with a constant normal force applied to the doubler by means of pulleys and weights as shown in the sketch of Fig. 5. Tests were performed with both tension and compression normal loads applied. Compression normal loads were obtained by passing cords through holes in the first doubler and attaching to the inside of the opposite doubler.

Cyclic Fatigue Tests

The fatigue tests were conducted at one cycle per second with a fully reversed ($R = -1$) sinusoidal load cycle. This was

the fastest practical cycling rate with the available test equipment due to the large stroke length required to obtain the desired load levels. Cyclic loading was begun at a low load level to prevent shock loading the material and then the load increased to the test level. Test stress levels were reached in less than 25 cycles. During the tests, the lateral movement of the specimen was monitored using a dial gage to ensure that the specimen was aligned. The load waveform was monitored using an oscilloscope to ensure that all specimens received the same loading cycle. The cyclic tests were stopped periodically and a single stress-strain cycle was conducted at 0.1 cps to monitor changes in SIP stiffness and permanent SIP extension.

Results and Discussion

The results that will be presented in the following sections are based on a limited number of tests. The test results were often obtained from the same lot of material. Since the material is known to have fairly wide variations in the material properties between lots, the results should be viewed as showing trends and approximate values only. Many more tests and material lots are needed to define statistically valid material properties.

Tension/Compression Test Results¹

Stress-Strain Response

Typical stress-strain curves are shown in Fig. 6 for the 0.41 cm (0.160 in.) thick SIP. Curves are shown for the proof test, the first cycle after proof, and the 100th load conditioning cycle. The material is highly nonlinear in both tension and compression and the nonlinearity in tension becomes more severe with load cycles. Thus, the material is highly sensitive to previous load history. A large low modulus region exists near zero stress where small tension or compression stresses results in large strains; whereas, at the higher stress levels, changes in stress result in relatively small changes in strain. The constant load interval during the proof loading results in considerable creep of the material in tension, but very little creep in compression. Removal of the proof load does not return the specimen to its original condition but results in a permanent strain of approximately 15%. The first cycle after proof results in a tensile strain that is much larger than was obtained for the same stress level during the proof. The 100th cycle results in a larger tensile strain than was obtained during the proof test, even at the higher stress level. The compression stress-strain relationship does not change significantly with load cycles. The material has high hysteresis as evident by the large area enclosed by the stress-strain load/unload curves. The hysteresis decreases for the first cycle after the proof test, but does not decrease significantly beyond this for additional load cycles.

Tangent Modulus

The tension tangent modulus for the SIP is shown in Fig. 7 as a function of strain. For strain levels of 10% or less, the SIP has low modulus values which increase very rapidly at the higher strain levels. For the virgin material, the modulus increases almost linearly with strain. Proof testing and load conditioning the SIP increases the extent of the low modulus region and greatly increases the tangent modulus at the higher strains. The highly nonlinear nature of the SIP is shown by the large variations in the tensile tangent modulus.

Ultimate Tensile Strength

Ultimate tensile strength data for several tests conducted on the 0.41 cm (0.160 in.) thick SIP are tabulated in Table 1. Data are given for both load and displacement controlled tests and for varying loading rates. The tensile ultimate strength varies between 201 kPa (29.1 psi) and 335 kPa (48.6 psi), with an average value of approximately 270 kPa (39 psi). The average value compares favorably with the 290 kPa (42 psi)

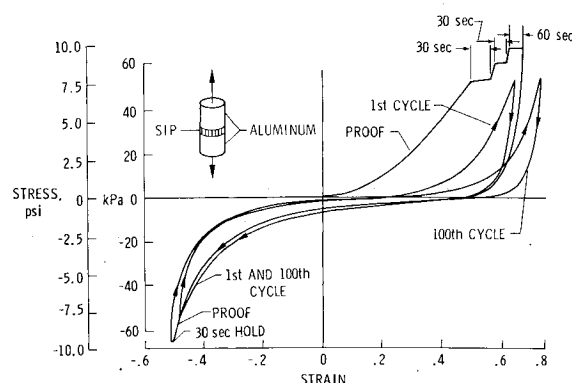


Fig. 6 Typical proof and load conditioning curves for 0.41 cm (0.16 in.) thick SIP. Proof load is 69 kPa (10 psi) and conditioning load is 80% of proof load.

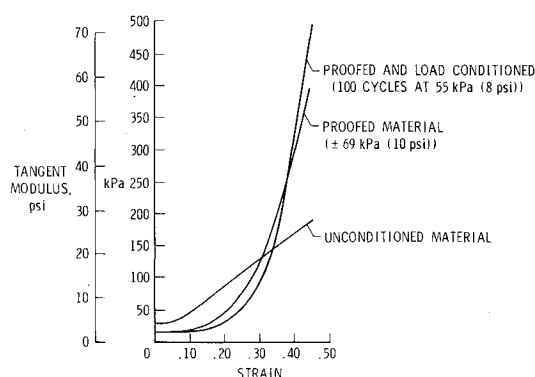


Fig. 7 Effect of proof cycle and load conditioning on tensile tangent modulus of 0.41 cm (0.16 in.) thick SIP.

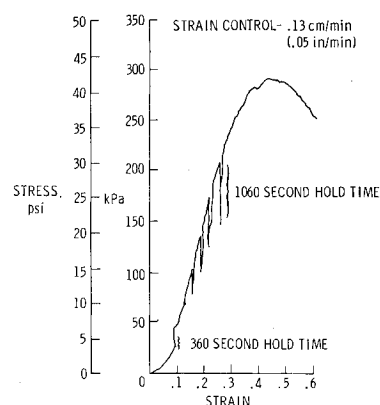


Fig. 8 Short time load relaxation response for the 0.41 cm (0.16 in.) thick SIP.

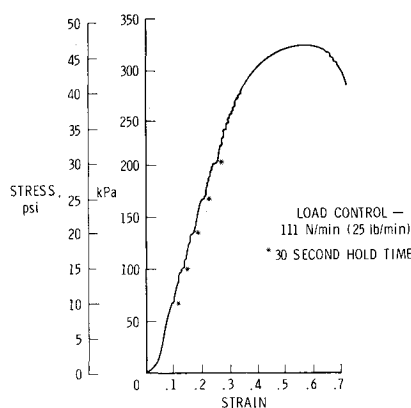
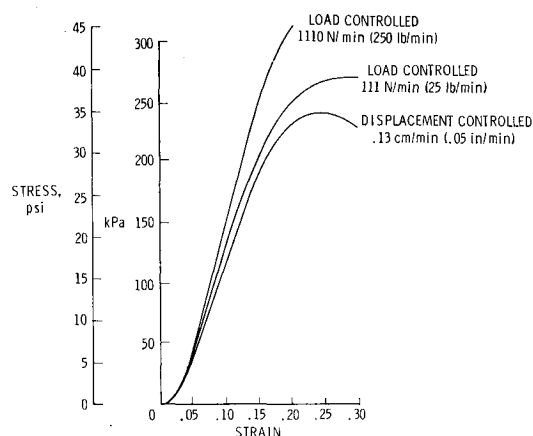
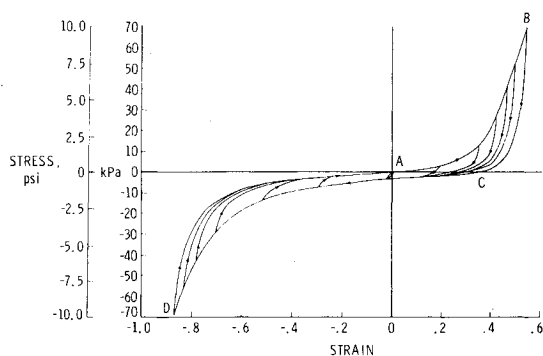
average value presented in Ref. 8 for the same material. A tenfold increase in the load rate or a fivefold increase in the displacement rate increases the measured ultimate tensile strength by approximately 20%. Load controlled tests tend to give slightly higher measured values of tensile ultimate strength than do displacement controlled tests.

Relaxation and Creep

Short time relaxation and creep response for the SIP are shown in Figs. 8 and 9, respectively. The relaxation curve was obtained by loading the specimen at a constant strain rate of 0.13 cm/min (0.05 in./min) and by holding the strain constant at several points until there was no noticeable additional relaxation of the stress within load application times of interest. The hold time varied from 360 s at the lowest strain

Table 1 Ultimate tensile strength data for several tests conducted on the 0.41 cm (0.160 in.) thick SIP

Displacement controlled			Load controlled		
Test no.	Rate	σ_{ult} kPa (psi) unconditioned material	Test no.	Rate	σ_{ult} kPa (psi) unconditioned material
2	0.13 cm/min	238 (34.5)	12	111 N/min	259 (37.6)
3		232 (33.7)	13		271 (39.3)
4	(0.5 in./min)	241 (35.0)	14	(25 lb/min)	323 (46.8)
5		201 (29.1)	16		267 (38.7)
Avg. =		229 (33.2)			280 (40.6)
6	0.64 cm/min	305 (44.3)	15	1110 N/min	335 (48.6)
7		256 (37.2)			
8	(0.25 in./min)	271 (39.3)		(250 lb/min)	
9		279 (40.4)			
10		265 (38.5)			
Avg. =		275 (39.9)			

**Fig. 9** Short time creep response for the 0.41 cm (0.16 in.) thick SIP.**Fig. 11** Typical tension stress-strain behavior for different load and strain rates. Material in virgin 0.41 cm (0.16 in.) thick SIP.**Fig. 10** Typical family of stress-strain curves for the 0.41 cm (0.16 in.) thick SIP that has been load conditioned for 100 cycles at ± 70 kPa (10 psi).

hold level of 0.10 to 1060 s at the highest strain hold level of 0.23. The stress relaxation becomes progressively larger for larger strains.

The curve showing creep was obtained by loading the specimen at a constant load rate of 110 N/min (25 lbs/min) and by holding the load constant at several stress levels for 30 s. For the short time observed, there was noticeable creeping of the material even at low stresses. Additional creep would be expected for longer hold time intervals, as it was not demonstrated that creep had stopped in the short time observed.

The sensitivity of the SIP material to previous load history and the hysteresis behavior of the SIP was noted in the discussion of Fig. 6. A typical hysteresis stress-strain loop is shown in Fig. 10 for the 0.41 cm (0.160 in.) thick SIP that has been load conditioned for 100 cycles at ± 70 kPa (10 psi). The outer closed loop ABCDA is the load/unload stress-strain curve for a stress level of ± 70 kPa (10 psi). Due to the hysteresis properties of the material, a family of stress-strain curves exist within the closed loop as shown by the inner curves in Fig. 10. Thus, the correct stress-strain curve to use in a particular application depends on the immediate stress-strain state of the material and the direction of loading as well as on the previous load conditioning history.

Load Rate

The effects of load rate on the stress-strain curves and ultimate strength for typical unconditioned SIP specimens are shown in Fig. 11. The lower curve was obtained with a displacement rate of 0.13 cm/min (0.05 in/min). The middle curve was obtained with a load rate of 111 N/min (25 lbs/min) and the upper curve with a load rate of 1110 N/min (250 lbs/min). Increasing the load rate results in the SIP having a higher ultimate strength as shown in Table 1 and the stress-strain curve having a higher tangent modulus at all stress levels. Although the 111 N/min (25 lbs/min) load controlled test and the displacement controlled test had approximately the same average head motion rate over most of the test range, the load controlled test had a higher tangent

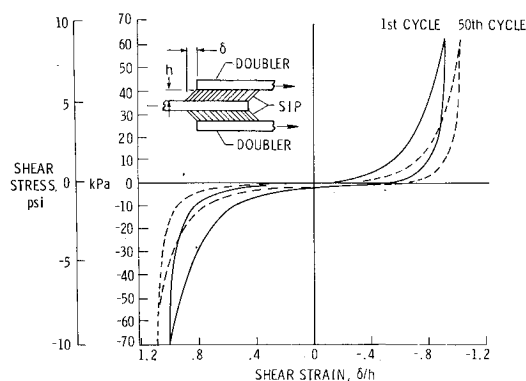


Fig. 12 Typical shear stress-strain behavior for 0.41 cm (0.16 in.) thick SIP in cross-roll direction.

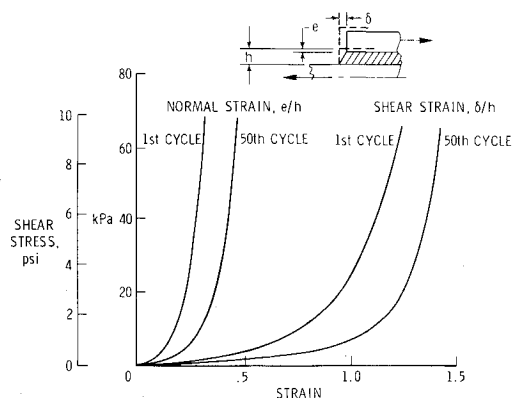


Fig. 13 Stress-strain behavior for unconditioned and load conditioned 0.41 cm (0.16 in.) thick SIP in cross-roll direction.

modulus and ultimate strength than the displacement controlled test.

Shear Test Results²

Typical shear stress-strain characteristics including results of cyclic loading to 50 cycles of the 0.41 cm (0.160 in.) thick SIP in the cross-roll direction are shown in Fig. 12 and have a form similar to the tension-compression stress-strain curves. The material is highly nonlinear, has a large shear hysteresis loop, is sensitive to previous load history, and has a large low shear modulus region for low stress levels. Strains normal to the shear plane are shown in Fig. 13, along with the shear strain for the SIP being loaded in shear. The material was load cycled for up to 50 cycles between ± 70 kPa (± 10.0 psi). The strain progressively increased for a given stress level because of a progressive increase in the extent of the low modulus region for the material. The effect of load conditioning on the shear tangent modulus is shown in Fig. 14.

As shown in Fig. 15, the SIP exhibits different stiffness characteristics in the roll and cross-roll directions, reflecting the preferred orientation imparted to the material by the needled roller during manufacturing. For a given stress level, the low modulus region is larger for the material stressed in the roll direction than in the cross-roll direction, thus resulting in larger strains in the roll direction. Normal strains are not significantly affected by the roll direction. Conditioning the material by load cycling has the same effect in both the roll and cross-roll direction.

Shear stress-strain curves obtained with either a small tension or compression transverse normal force applied to the material are shown in Fig. 16 for comparison with the shear stress-strain curves for the material without a transverse normal force. Either a tension or compression transverse normal force results in a reduction in the shear strain for a given stress level, thus indicating the coupling between the

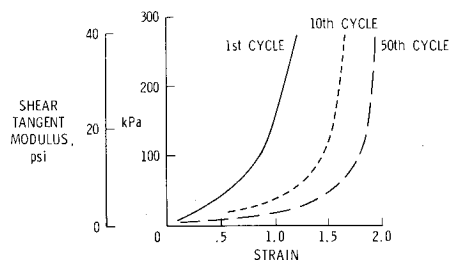


Fig. 14 Effect of load conditioning on shear tangent modulus of 0.41 cm (0.16 in.) thick SIP.

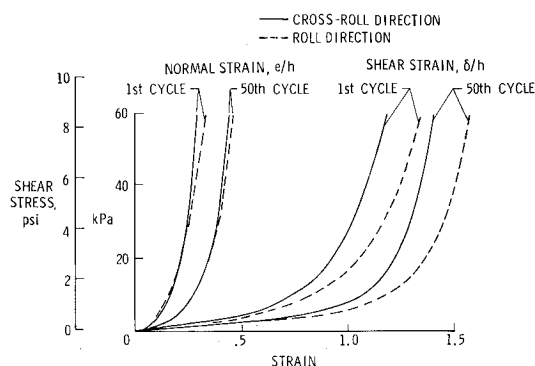


Fig. 15 Effect of material orientation on shear behavior of 0.41 cm (0.16 in.) thick SIP. Cyclic load level = 69 kPa (10 psi).

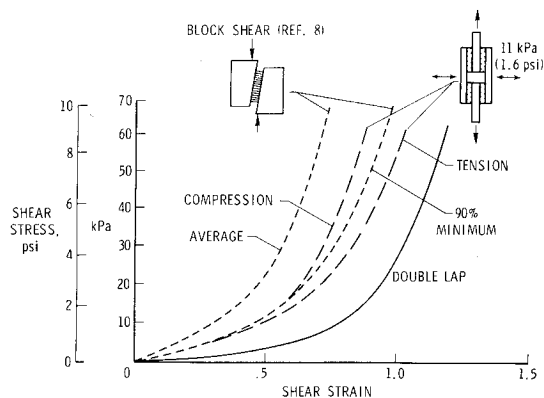


Fig. 16 Effect of normal force on shear behavior of 0.41 cm (0.16 in.) thick SIP in roll direction.

transverse normal and shear strains. The low shear stiffness of the SIP increases the importance of the coupling effect. Shear test results obtained in Ref. 8 using a block shear test specimen are shown in Fig. 16 for comparison with the present results. Two stress-strain curves obtained using block shear specimens are shown; one is an average curve and the other represents the minimum stiffness bounds for 90% of the specimens tested. The results show that the small transverse normal loads inherent in the block shear test specimen results in significantly smaller shear strains for a given stress level. Further, during flight when the tiles are subjected to transverse aerodynamic loads, the shear stiffness of the SIP can be expected to be greater than that measured in the laboratory. Thus, the test technique used in obtaining the shear information of the SIP should be considered in the design and analysis process.

Cyclic Fatigue Test Results³

A summary of the results of the cyclic fatigue tests for each SIP/tile system are shown in Fig. 17 for the 0.41 cm (0.160

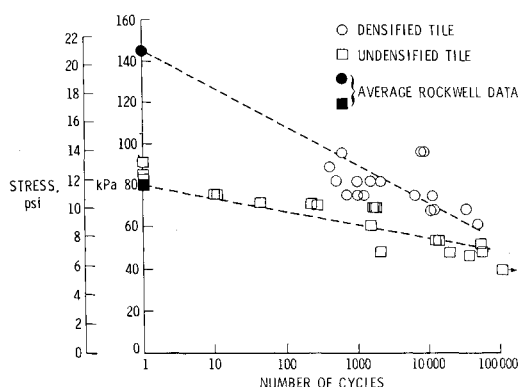


Fig. 17 Cyclic load tests of 0.41 cm (0.16 in) thick SIP/LI-900 densified and undensified tile system, $R = P1$.

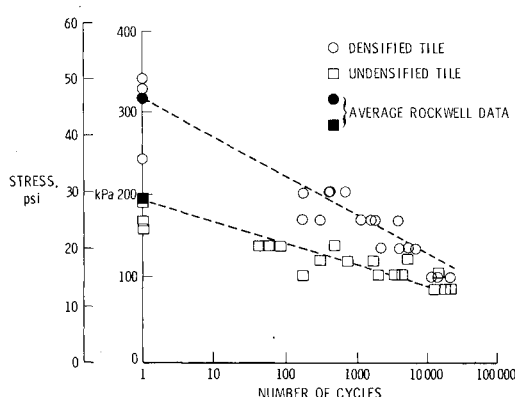


Fig. 18 Cyclic load tests of 0.23 cm (0.90 in) thick SIP/LI-2200 densified and undensified tile system, $R = -1$.

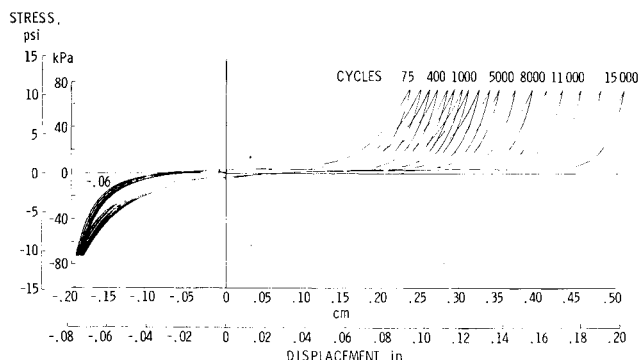


Fig. 19 Effect of cyclic loading on displacement of 0.41 cm (0.16 in) thick SIP/LI-900 densified tile system, $R = -1$.

in.) / LI-900 tile densified and undensified system, and Fig. 18 for the 0.23 cm (0.090 in.) / LI-2200 densified and undensified tile system. The stress levels are shown as a function of the number of fully reversed ($R = -1$) cycles to failure for each SIP/tile system. The dashed lines on each figure are a least squares fit of the test results where the intersection at one cycle (indicated by the filled symbols) is the mean static failure stress of at least 45 tests performed by Rockwell International, the prime contractor for the shuttle orbiter. A small number of static tests were performed during the current fatigue program and results are plotted at the one cycle location.

Cyclic loading results in a relatively large reduction in the stress level that each of the SIP/tile systems can withstand for a small number of cycles. For example, the average static

strength of the 0.41 cm (0.160 in.) thick SIP/LI-900 undensified tile system (see square symbols in Fig. 17) is reduced from 86 kPa (12.5 psi) to 62 kPa (9 psi) after a thousand cycles. Although the 0.23 cm (0.090 in.) thick SIP/LI-2200 undensified tile system has a higher strength (see square symbols in Fig. 18), similar reductions in fatigue strength are obtained. Both of the undensified tile systems have a SIP/tile interface failure mode. Densifying the faying surface of the RSI tile strengthens the SIP/tile interface sufficiently that cyclic loading failure occurs in the SIP due to complete failure or excessive elongation. Figure 19 shows typical load deflection curves for the 0.41 cm (0.160 in.) thick SIP after various load cycles. Each load cycle results in slightly increased elongation of the SIP during the tension portion of the cycle until complete separation failure occurs. Failure of the TPS due to the excessive elongation of the SIP may occur before complete separation.

For the 0.41 cm (0.160 in.) thick SIP/LI-900 densified tile system shown by the circle symbols in Fig. 17, failure of the SIP was arbitrarily assumed to have occurred when the elongation between the maximum and minimum loads exceeded 0.64 cm (0.25 in.). Once the total elongation reaches 0.64 cm (0.25 in.), the specimen rapidly deteriorates under further load cycling until complete SIP separation failure occurs. For the 0.23 cm (0.090 in.) thick SIP/LI-2200 densified tile system shown by the circle symbols in Fig. 18, the data points represent complete failures of the SIP material. If a more restrictive elongation criteria is chosen as a failure condition for either SIP/tile system, the degradation in system fatigue strength due to cyclic loading would be more severe.

Densification of the faying surface increases both the static and fatigue strength of each SIP/tile system. The 0.41 cm (0.160 in.) thick SIP/LI-900 densified tile system at 69 kPa (10 psi) has a mean lifetime of approximately 15,000 cycles, whereas the same system undensified has an expected lifetime of only 100 cycles at the same stress level. Similarly, the 0.23 cm (0.090 in.) thick SIP/LI-2200 densified tile system at 138 kPa (20 psi) has a mean lifetime of approximately 8,000 cycles, whereas the same system undensified has an expected mean lifetime of only 200 cycles at the same stress level. However, even the densified tile systems have a relatively low fatigue life due to excessive elongation or complete failure of the SIP. Thus the full benefit of the increased static strength of the densified tile system is not achieved in fatigue. Also, since failure occurs due to SIP elongation, further improvements in the RSI tile strength alone will not result in any improvement in the total system fatigue strength.

Concluding Remarks

An experimental investigation has been conducted to determine the static and fatigue properties of the Strain Isolator Pad (SIP) used on the shuttle orbiter Thermal Protection System (TPS). Transverse tension, compression, and shear test results show that the SIP is highly nonlinear, has a large hysteresis, has a large low modulus region for low stress levels, and is highly sensitive to strain rates and previous load history. The transverse shear properties are also sensitive to transverse normal forces and to the orientation of the material. Due to the hysteretic nature of the material, the correct stress-strain curve to use in a particular application depends on the immediate stress-strain state of the material and the direction of loading as well as on the previous load conditioning history. For the undensified tile systems, both static and fatigue failure occur at the SIP/tile interface at low stress levels and for a small number of cycles. Densifying the faying surface of the tile improves the static and fatigue strength of the SIP/tile system, but cyclic loading causes a deterioration of the SIP which results in a relatively low fatigue life due to excessive elongation or complete failure of the SIP. Thus, the full benefit of the increased static strength

of the densified tile system is not achieved in fatigue. Also, further improvement in the RSI tile strength will not result in any improvements in the total system fatigue strength.

References

¹Sawyer, J. W. and Rummler, D. R., "Room Temperature Mechanical Properties of Shuttle Thermal Protection System Materials," NASA TM-81786, April 1980.

²Sawyer, J. W. and Waters, W. A., Jr., "Room Temperature Shear Properties of the Strain Isolator Pad for the Shuttle Thermal Protection System," NASA TM-81900, Jan. 1981.

³Sawyer, J. W. and Cooper, P. A., "Fatigue Properties of Shuttle Thermal Protection System," NASA TM-81899, Nov. 1980.

⁴Ransone, P. O. and Rummler, D. R., "Microstructural Characterization of the HRSI Thermal Protection System for Space Shuttle," NASA TM-81821, May 1980.

⁵Prabhakaran, R. and Cooper, P. A., "Photoelastic Tests on Models of Thermal Protection System for Space Shuttle Orbiter," NASA TM-81866, Aug. 1980.

⁶Cooper, P. A. and Holloway, P. F., "The Shuttle Tile Story," *Astronautics and Aeronautics*, Vol. 19, Jan. 1981.

⁷Korb, L. J. and Clancy, H. M., "Shuttle Orbiter Thermal Protection System: A Material and Structural Overview," presented at the 26th National Symposium Society for the Advancement of Materials and Process Engineering, Los Angeles, Calif., April 28-30, 1981.

⁸Rockwell International, Materials Property Manual, Vol. 3, *Thermal Protection System Materials Data*, Rockwell International Publication, Pu. 2543-W, Rev. 5-79, May 1979.

From the AIAA Progress in Astronautics and Aeronautics Series..

OUTER PLANET ENTRY HEATING AND THERMAL PROTECTION—v. 64

THERMOPHYSICS AND THERMAL CONTROL—v. 65

Edited by Raymond Viskanta, Purdue University

The growing need for the solution of complex technological problems involving the generation of heat and its absorption, and the transport of heat energy by various modes, has brought together the basic sciences of thermodynamics and energy transfer to form the modern science of thermophysics.

Thermophysics is characterized also by the exactness with which solutions are demanded, especially in the application to temperature control of spacecraft during long flights and to the questions of survival of re-entry bodies upon entering the atmosphere of Earth or one of the other planets.

More recently, the body of knowledge we call thermophysics has been applied to problems of resource planning by means of remote detection techniques, to the solving of problems of air and water pollution, and to the urgent problems of finding and assuring new sources of energy to supplement our conventional supplies.

Physical scientists concerned with thermodynamics and energy transport processes, with radiation emission and absorption, and with the dynamics of these processes as well as steady states, will find much in these volumes which affects their specialties; and research and development engineers involved in spacecraft design, tracking of pollutants, finding new energy supplies, etc., will find detailed expositions of modern developments in these volumes which may be applicable to their projects.

Volume 64—404 pp., 6 × 9, illus., \$20.00 Mem., \$35.00 List
Volume 65—447 pp., 6 × 9, illus., \$20.00 Mem., \$35.00 List
Set—(Volumes 64 and 65) \$40.00 Mem., \$55.00 List

TO ORDER WRITE: Publications Order Dept., AIAA, 1633 Broadway, New York, N.Y. 10019